JACS
JOURNAL OF THE AMERICAN CHEMICAL SOCIETY
Communication
pubs.acs.org/JACS

Giant Zn_{14} Molecular Building Block in Hydrogen-Bonded Network with Permanent Porosity for Gas Uptake

Suvendu Sekhar Mondal,[†] Asamanjoy Bhunia,[‡] Alexandra Kelling,[†] Uwe Schilde,[†] Christoph Janiak,*[,‡] and Hans-Jürgen Holdt*[,†]

[†]Institut für Chemie, Anorganische Chemie, Universität Potsdam, Karl-Liebknecht-Straße 24-25, 14476 Potsdam, Germany
[‡]Institut für Anorganische Chemie und Strukturchemie, Heinrich-Heine-Universität Düsseldorf, Universitätsstraße 1, 40225 Düsseldorf, Germany

Supporting Information

ABSTRACT: *In situ* imidazolate-4,5-diamide-2-olate linker generation leads to the formation of a $[Zn_{14}(L2)_{12}(O)(OH)_2(H_2O)_4]$ molecular building block (MBB) with a Zn_6 octahedron inscribed in a Zn_8 cube. The MBBs connect by amide−amide hydrogen bonds to a 3D robust supramolecular network which can be activated for N_2, CO_2, CH_4, and H_2 gas sorption.

Supramolecular chemistry is of great interest in the design of new solid-state materials because it takes advantage of self-assembly to synthesized new materials by virtue of cooperative interactions such as ion−ion interactions, hydrogen bonding, dipole−dipole interactions, and aromatic $\pi-\pi$ interaction.[1] Porous materials such as metal−organic frameworks (MOFs) receive increasing attention due to their potential applications in gas adsorption and separation, as molecular sieves, catalysts, sensors, and for drug release.[2]

Hydrogen-bonded molecular building blocks (MBBs) with permanent porosity are a new class of zeolite-like supramolecular materials. The groups of Beatty[3,4] and Eddaoudi[5,6] demonstrated that the use of metal−organic building blocks containing peripheral H-bonding substituents is an effective way to construct H-bonded supramolecular networks with channels and pores. The H-bonded 3-D assembly, MOC-2 (MOC = metal−organic cube), was formed under solvothermal conditions using $In(NO_3)_3{\cdot}6H_2O$ and 4,5-dicyanoimidazole ($(CN)_2Im$) as the precursor for the *in situ* generation of the protonated 4,5-imidazolatedicarboxylate ligand (HImDC) by complete hydrolysis of the cyano groups of $(CN)_2Im$.[5]

We previously developed a new class of metal−organic frameworks called IFPs (IFP = imidazolate framework Potsdam) based on 2-substituted imidazolate-4-amide-5-imidate linkers.[7−9] The chelating linker, 2-substituted imidazolate-4-amide-5-imidate, was generated *in situ* by partial hydrolysis of 2-substituted $(CN)_2Im$ in the presence of a metal salt hydrate in *N,N′*-dimethylformamide (DMF) under solvothermal conditions.

Here, we describe a supramolecular network (**1**) based on a Zn_{14}-MBB which is formed from *in situ* hydrolysis of the ligand precursor 4,5-dicyano-2-methoxyimidazole (L1). Partial hydrolysis of the cyano groups to amide groups and of the methoxy to the hydroxy group followed by two-fold deprotonation generates the imidazolate-4,5-diamide-2-olate linker (L2) (Schemes 1 and S2 (Supporting Information)). The ligand L2 is only stable in the deprotonated and metal-coordinated state.

Scheme 1. *In Situ* Imidazolate-4,5-diamide-2-olate (L2) Linker Synthesis, with Indication of Its Zinc Coordination (cf. Figure 1a) and Hydrogen Bonds in 1 (See Supporting Information for experimental details)

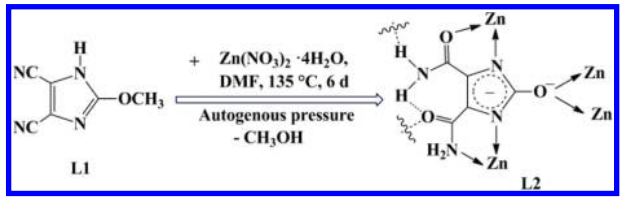

Compound **1** belongs to the hexakisoctahedric crystal class ($m\bar{3}m$) within the cubic crystal system, and a rhombic dodecahedron is formed. Single crystals show 12 faces (Figure S1). The space group is $Ia\bar{3}d$ (No. 230), possessing the highest crystallographic symmetry. As-synthesized **1** was characterized by single-crystal X-ray diffraction as $[Zn_{14}(L2)_{12}(O)(OH)_2(H_2O)_4](DMF)_{18}$.[11] Twelve L2 ligands, one oxide ion, two hydroxide ions, and four water molecules assemble with 14 zinc ions to an unprecedented cube-like tetradecanuclear Zn_{14}-MBB with peripheral amide groups (Figure 1b). The zinc atoms in the Zn_{14} cluster form a distorted Zn_8 cube (Zn2 and Zn3 with an inscribed Zn_6 octahedron (Zn1). The bridging action between the Zn atoms is based on the dianionic imidazolate-olate part of the L2 linker and the oxide ion. The oxide ion (O1) is located in the center of the MBB, surrounded by six Zn1 atoms in an exact octahedral coordination environment (Figure S6b). Terminal water and hydroxide ligands conclude the Zn1 octahedral coordination sphere. Moreover, the combination of three different types of coordination environments (octahedral for Zn1, tetrahedral for Zn2, and distorted trigonal prismatic for Zn3) around the Zn atoms in one compound is rarely observed (see Supporting Information).[12]

The MBB contains amide groups at its vertices and edges. Each cubic-like MBB is connected through its vertices with

Received: October 16, 2013
Published: December 7, 2013

   dx.doi.org/10.1021/ja410595q | *J. Am. Chem. Soc.* 2014, 136, 44−47

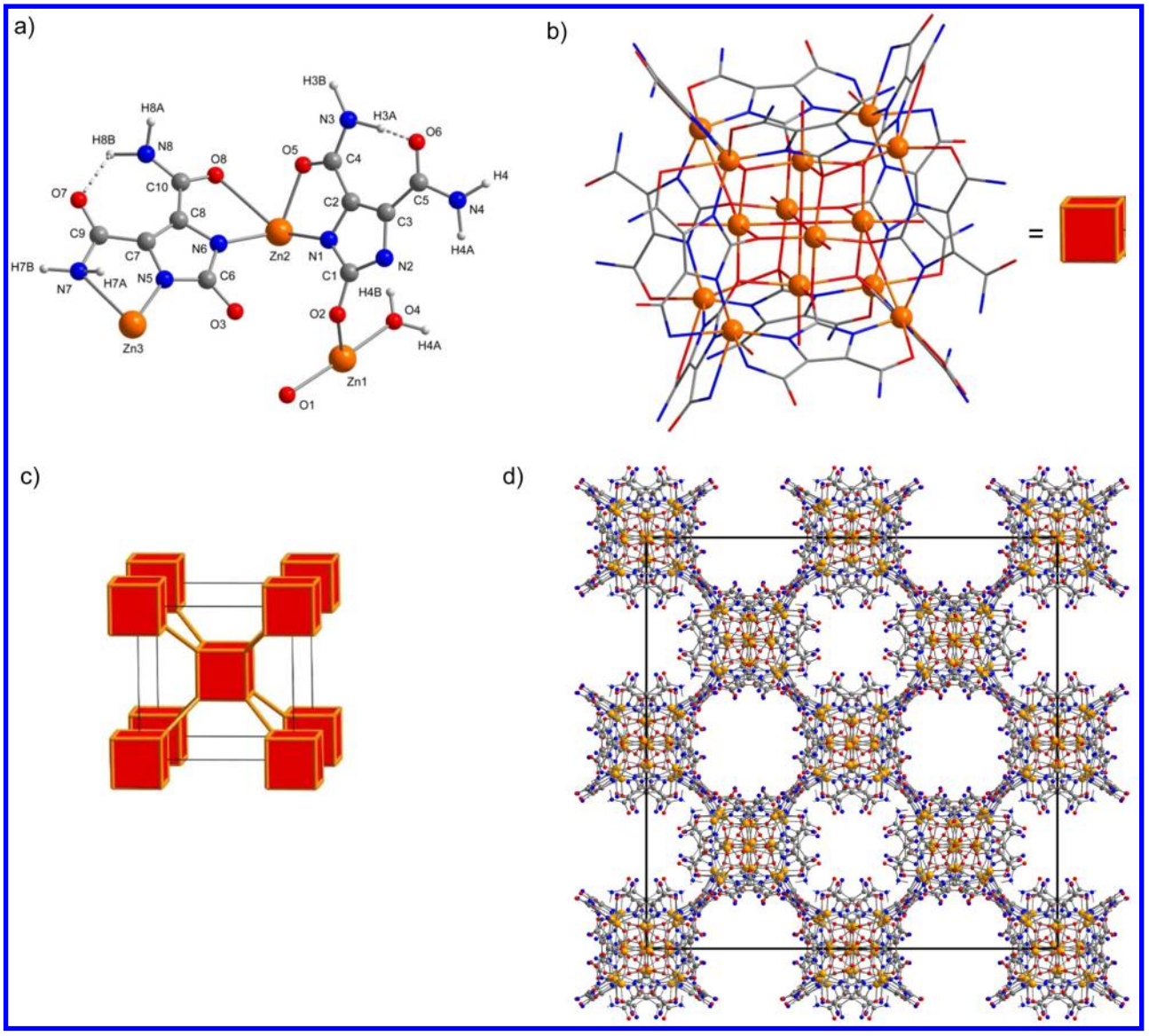

Figure 1. Crystal structure of **1**: (a) asymmetric unit, (b) tetradecanuclear zinc MBB (hydrogen atoms are omitted for clarity), (c) schematic presentation of the supramolecular augmented body-centered cubic arrangement of the MBBs, and (d) hydrogen-bonded supramolecular assembly of **1** (without hydrogen atoms).

eight MBBs in a body-centered cubic packing (Figure 1c) by intermolecular N−H···O hydrogen bonds between the peripheral amide groups, generating the 3D supramolecular assembly of **1** (Figure 1d). Previously reported azolate-based building blocks are connected via H-bonds with carboxylate groups.[5,6] To the best of our knowledge, **1** is the first example where amide groups of MBBs are engaged in H-bonding among azolate-based building blocks.

The topology of **1** can be described as H-bonded eight-center body-centered cubic (**bcu**) net with the nodes as Zn_{14}-MBBs (Figure 1c). Alternatively, since the Zn_{14}-MBB could be described as a cube, one can also describe the net as the augmented version of **bcu** (= **bcu-a**) that is called polycubane (**pcb**).[13] Inspection of the reference codes for H-bonded **bcu** nets in TOPOS[14] revealed that metal-based nodes contain only two, four, and eight metal atoms,[5,15] whereas the **bcu**-net of **1** contains 14 Zn atoms of **bcu**-net family.

The degree of *in situ* hydrolysis of the cyano groups of 4,5-dicyano-2-methoxyimidazole (L1) into the corresponding imidazolate-4,5-diamide-2-olate (L2) was studied with infrared (IR) spectroscopy. The IR spectrum of the **1** manifests no stretching bands related to C≡N in the region of 2225−2240 cm^{-1}. Instead, the typical absorption bands for an amide are observed between 3450 and 3200 cm^{-1} and at 1658 and 1548 cm^{-1} (Figure S2). Moreover, the solid-state magic-angle-spinning (MAS) ^{1}H and ^{13}C NMR spectra of as-synthesized **1** (Figure S3) shows the ^{1}H and ^{13}C MAS NMR signals of the imidazolate-4,5-diamide-2-olate linker. The purity of the as-synthesized material was confirmed by elemental anaylsis, solid-state NMR spectra (Figure S3), and positive matching between simulated and experimental powder X-ray diffraction (PXRD) patterns (Figure S5).

The framework of **1** exhibits two types of infinite channels. The first type of channel has small openings with an approximate diameter of 3.9 Å, while the second type can accommodate a sphere with a maximum diameter of 6.0 Å, given the van der Waals radii of the nearest atoms (Figure S8).

dx.doi.org/10.1021/ja410595q | *J. Am. Chem. Soc.* 2014, 136, 44−47

The peripheral amide groups of the MBBs which are not involving in H-bonds point into the channels.

The channels of as-synthesized **1** contain three DMF molecules per formula unit, with solvent-accessible void volume of 53% of the unit cell volume (see SI for details). Solid-state NMR spectroscopy of as-synthesized **1** also provided evidence for the presence of DMF molecules. Solvent exchange was carried out by Soxhlet extraction with dry methanol over 7 days. The solvent-exchanged material was activated by degassing at 50 °C under high vacuum (10^{-6} Torr) for 24 h, prior to gas-sorption measurements. This activation procedure completely removed the DMF molecules, as confirmed by liquid-phase ^{13}C NMR spectroscopy (Figure S4). Moreover, the activated sample maintained its crystalline integrity, as indicated in the PXRD pattern (Figure S5).

The N_2 adsorption/desorption isotherms at 77 K exhibit type-IV characteristics with a hysteresis loop which is associated with capillary condensation taking place (Figure 2a). N_2 sorption measurements were reproducibly carried out three times on the same probe to ensure retention of porosity. There is a limiting uptake over a range of high p/p_0.[16] The desorption shows an H2-type hysteresis loop in the 0.4−1.0 p/p_0 range which may be attributed to a difference in mechanism between condensation and evaporation processes occurring in pores with narrow necks and wide cavities.[16] The estimated Brunauer−Emmett−Teller (BET) surface area and the Langmuir surface area are 471 m^2/g and 570 m^2/g, respectively. However, such surface areas are slightly higher than those of azolate-based supramolecular assemblies (MOC-3[5] and ZSA-2[6]) and higher than those of some H-bonded porous organic networks (SOF-1a,[17a] HOF-1a,[17b] CBDU,[17c] and TTEB[17d]).

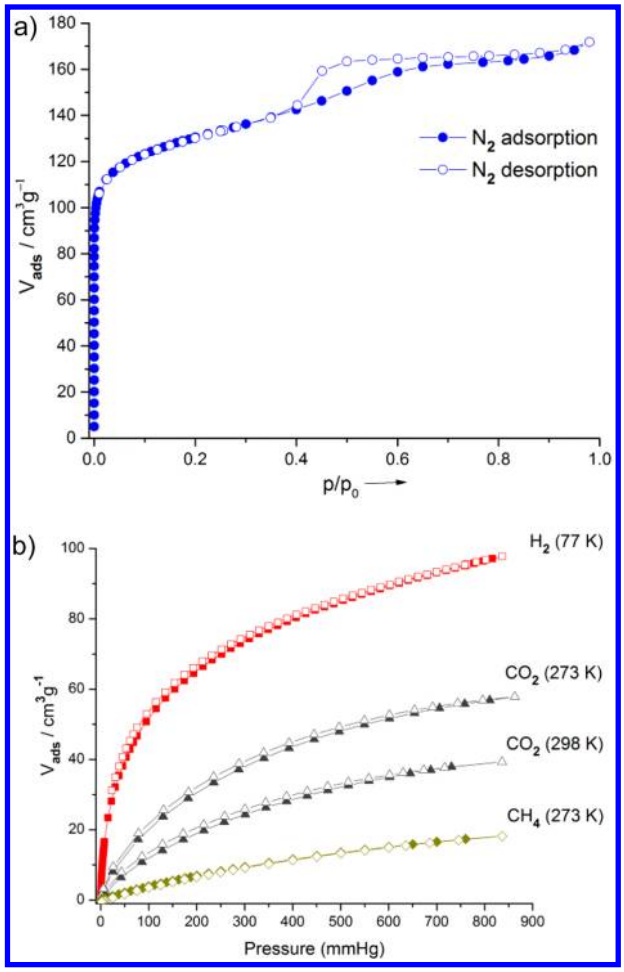

Figure 2. (a) N_2 sorption isotherm at 77 K and 1 bar of **1**; (b) H_2, CO_2, and CH_4 isotherms at 1 bar. Adsorption and desorption branches are indicated in closed and open symbols, respectively.

The total pore volume was 0.26 cm^3/g (from "N_2 DFT slit pore" model of N_2 sorption data at 77 K), which is less than the 0.42 cm^3/g based on the PLATON-calculated 53% void volume.[18] However, at cryogenic temperature, diffusion of N_2 molecules into small micropores is very slow. This diffusion limitation at 77 K influences N_2 adsorption in ultramicropores (pores smaller than 7 Å) so that N_2 probably does not probe the 3.9 Å channels.[19] The CO_2 adsorption capacities in activated **1** are 56 cm^3/g at 273 K and 38 cm^3/g at 298 K (Figure 2b). Desorption branches show a slight H4-type hysteresis which is often associated with narrow slit-like pores.[16] At 273 K and under higher absolute pressures, CO_2 molecules can more easily access ultramicropores than N_2 at ~77 K, and the kinetic diameter of CO_2 (3.3 Å) is also a little bit smaller than for N_2 (3.64 Å). So, advantages of micropore analysis by CO_2 adsorption at 273 K versus N_2 adsorption at 77 K are (i) faster analysis, (ii) greater confidence that measured adsorption points are equilibrated (both due to higher diffusion rates), and (iii) extension of the range of analysis to pores of smaller sizes that are accessible to CO_2 molecules but not to N_2.[20] From the CO_2 adsorption isotherm at 273 K, the pore size distribution was derived between 4 and 10 Å by using NLDFT with a "CO_2 on carbon-based slit-pore model" (Figure S12) and showed a relative maximum at ~5.6 Å which is comparable with the larger channel diameter (6.0 Å) obtained from the X-ray structure. The CO_2 uptake of **1** at 298 K and 1 bar was comparable to ZIF-68 (37.6 cm^3/g), ZIF-69 (40.6 cm^3/g), ZIF-79 (33.5 cm^3/g), and ZIF-81 (38.2 cm^3/g, ZIF = zeolitic imidazolate framework) which have, however, about twice the BET surface area of **1** (see Table S7).[21] The fact that relatively large amounts of CO_2 are adsorbed in the comparatively low-surface-area material of **1** suggests that CO_2 interacts with the amide-functionalized framework due to its large polarizability and quadrupole moment. To further understand the adsorption properties, the isosteric heats of adsorption were calculated from the CO_2 adsorption isotherms at 273 and 298 K (Figure S13). At zero loading the Q_{st} value ($-\Delta H$) is 38 kJ/mol. Upon increasing the loading the Q_{st} value decreases rapidly to 28 kJ/mol which is still well above the heat of liquefaction of bulk CO_2 with 17 kJ/mol. The high Q_{st} value can be attributed to the high polar framework and the pore size effect. The high adsorption enthalpy at zero coverage is explained by the initial filling of the small ultramicropores with 4 Å diameter (Figure S8) with adsorbate−surface interactions to both sides or ends of the CO_2 molecules. The methane sorption capacity for **1** at 273 K was estimated to be 17.3 cm^3/g (Figure 2b). **1** adsorbs 95.1 cm^3/g (or 0.85 wt %) H_2 at 77 K and 1 bar (Figure 2b). Such uptake capacity is higher than those of dicarboxlate-azolate-based supramolecular assemblies like ZSA-1 and ZSA-2, measured at 298 K and 80 bar.[6]

In conclusion, we have reported an *in situ* linker generation method for the synthesis of new molecular building blocks that are connected by hydrogen bonds into a porous supramolecular network. The ditopic linker was designed in such a way that it simultaneously acts as bridging and capping ligand, which is necessary for supramolecular assemblies via predictable N−H···O hydrogen bonds. Interestingly, **1** crystallizes in the most

dx.doi.org/10.1021/ja410595q | *J. Am. Chem. Soc.* 2014, 136, 44−47

symmetrical space group, $Ia\bar{3}d$ (No. 230), which is very rare for organic and metal−organic compounds. N_2, CO_2, and H_2 uptake capacities are higher than those reported for azolate-based hydrogen-bonded supramolecular assemblies and hydrogen-bonded porous organic compounds and ZIFs.

■ ASSOCIATED CONTENT

Supporting Information

Experimental details, characterization data, crystallographic data (CIF), and additional tables and figures. This material is available free of charge via the Internet at http://pubs.acs.org.

■ AUTHOR INFORMATION

Corresponding Authors

janiak@uni-duesseldorf.de
holdt@uni-potsdam.de

Notes

The authors declare no competing financial interest.

■ ACKNOWLEDGMENTS

Authors gratefully thank Prof. Vladislav A. Blatov (Department of Chemistry, Samara State University, Russia) and Prof. Davide M. Proserpio (Department of Structural Chemistry DCSSI, Università degli Studi di Milano, Italy) for helpful discussions concerning the nets and Prof. C. Jäger (BAM Federal Institute for Materials Research and Testing, Berlin, Germany) for solid-state NMR measurements. This work is financially supported by the Priority Program 1362 of the German Research Foundation on "Metal−Organic Frameworks".

■ REFERENCES

(1) (a) Steed, J. W.; Atwood, J. L. *Supramolecular Chemistry*; Wiley-VCH: Weinheim, Germany, 2009. (b) Aakeröy, C.; Champness, N. R.; Janiak, C. *CrystEngComm* **2010**, *12*, 22−43.

(2) (a) MacGillivray, L. R. *Metal-Organic Frameworks: Design and Application*; John Wiley & Sons: Hoboken, NJ, 2010. (b) Farrusseng, D. *Metal-Organic Frameworks Applications from Catalysis to Gas Storage*; Wiley-VCH: Weinheim, Germany, 2011.

(3) Chen, C.-L.; Beatty, A. M. *J. Am. Chem. Soc.* **2008**, *130*, 17222−17223.

(4) Hogan, G. A.; Rath, N. P.; Beatty, A. M. *Cryst. Growth Des.* **201**, *11*, 3740−3743.

(5) Sava, D. F.; Kravtsov, V. Ch.; Eckert, J.; Eubank, J. F.; Nouar, F.; Eddaoudi, M. *J. Am. Chem. Soc.* **2009**, *131*, 10394−10396.

(6) Wang, S.; Zhao, T.; Li, G.; Wojtas, L.; Huo, Q.; Eddaoudi, M.; Liu, Y. *J. Am. Chem. Soc.* **2010**, *132*, 18038−18041.

(7) Debatin, F.; Thomas, A.; Kelling, A.; Hedin, N.; Bacsik, Z.; Senkovska, I.; Kaskel, S.; Junginger, M.; Müller, H.; Schilde, U.; Jäger, C.; Friedrich, A.; Holdt, H.-J. *Angew. Chem., Int. Ed.* **2010**, *49*, 1258−1262.

(8) Debatin, F.; Behrens, K.; Weber, J.; Baburin, I. A.; Thomas, A.; Schmidt, J.; Senkovska, I.; Kaskel, S.; Kelling, A.; Hedin, N.; Bacsik, Z.; Leoni, S.; Seifert, G.; Jäger, C.; Günter, C.; Schilde, U.; Friedrich, A.; Holdt, H.-J. *Chem.—Eur. J.* **2012**, *18*, 11630−11640.

(9) Mondal, S. S.; Bhunia, A.; Baburin, I. A.; Jäger, C.; Kelling, A.; Schilde, U.; Seifert, G.; Janiak, C.; Holdt, H.-J. *Chem. Commun.* **2013**, *49*, 7599−7601.

(10) Keene, T. D.; Price, D. J.; Kepert, C. J. *Dalton Trans.* **2011**, *40*, 7122−7126.

(11) Crystal data for **1**: $C_{10}H_{9.67}N_8O_{7.17}Zn_{2.33}$, M_r = 509.12 g/mol, crystal dimensions 0.50 × 0.45 × 0.40 mm, cubic, space group $Ia\bar{3}d$ (No. 230), $a = b = c$ = 40.1873(12) Å, V = 64903(6) Å^3, Z = 96, ρ_{calcd} = 1.25 g/cm^3; μ(Mo Kα) = 2.10 mm^{-1} (λ = 0.71073 Å), T = 210 K; $2\theta_{max}$ = 25.00°, 31 851 reflections measured, 4761 unique (R_{int} = 0.06543), R_1 = 0.0586, wR = 0.1540 ($I > 2\sigma(I)$).

(12) Anantharaman, G.; Roesky, H. W.; Magull, J. *Angew. Chem., Int. Ed.* **2002**, *41*, 1226−1229.

(13) (a) Baburin, I. A.; Blatov, V. A.; Carlucci, L.; Ciani, G.; Proserpio, D. M. *CrystEngComm* **2008**, *10*, 1822−1838. (b) Blatov, V. A.; Carlucci, L.; Ciani, G.; Proserpio, D. M. *CrystEngComm* **2004**, *6*, 377−395. (c) Baburin, I. A. *Z. Kristallogr.* **2008**, *223*, 371−381.

(14) Blatov, V. A. *IUCr CompComm Newsl.* **2006**, *7*, 4−38.

(15) O'Keeffe, M.; Peskov, M. A.; Ramsden, S. J.; Yaghi, O. M. *Acc. Chem. Res.* **2008**, *41*, 1782−1789. http://rcsr.anu.edu.au

(16) Sing, K. S. W.; Everett, D. H.; Haul, R. A.; Moscou, L.; Pierotti, R. A.; Rouquérol, J.; Siemieniewska, T. *Pure Appl. Chem.* **1985**, *57*, 603−619.

(17) (a) Yang, W.; Greenaway, A.; Lin, X.; Matsuda, R.; Blake, A. J.; Wilson, C.; Lewis, W.; Hubberstey, P.; Kitagawa, S.; Champness, N. R.; Schröder, M. *J. Am. Chem. Soc.* **2010**, *132*, 14457−14469. (b) He, Y.; Xiang, S.; Chen, B. *J. Am. Chem. Soc.* **2011**, *133*, 14570−14573. (c) Dewal, M. B.; Lufaso, M. W.; Hughes, A. D.; Samuel, S. A.; Pellechia, P.; Shimizu, L. S. *Chem. Mater.* **2006**, *18*, 4855−4864. (d) Msayib, K. J.; Book, D.; Budd, P. M.; Chaukura, N.; Harris, K. D. M.; Helliwell, M.; Tedds, S.; Walton, A.; Warren, J. E.; Xu, M.; McKeown, N. B. *Angew. Chem., Int. Ed.* **2009**, *48*, 3273−3277.

(18) Spek, A. L. *PLATON: A Multipurpose Crystallographic Tool*; Utrecht University: Utrecht, The Netherlands, 2001.

(19) Rodriguez-Reinoso, F.; Linares-Solano, A. In *Chemistry and Physics of Carbon*; Thrower, P. A., Ed.; Marcel Dekker: New York, 1988; Vol. *21*.

(20) (a) Garrido, J.; Linares-Solano, A.; Martin-Martinez, J. M.; Molina-Sabio, M.; Rodriguez-Reinoso, F.; Torregosa, R. *Langmuir* **1987**, *3*, 76−81. (b) Cazorla-Amoros, D.; Alcaniz-Monje, J.; Linares-Solano, A. *Langmuir* **1996**, *12*, 2820−2824. (c) Garcia-Martinez, J.; Cazorla-Amoros, D.; Linares-Solano, A. In *Characterization of Porous Solids V*; Unger, K. K., Kreysa, G., Baselt, J. P., Eds.; Elsevier: Amsterdam, 2000; pp 485−494.

(21) Banerjee, R.; Furukawa, H.; Britt, D.; Knobler, C.; O'Keeffe, M.; Yaghi, O. M. *J. Am. Chem. Soc.* **2009**, *131*, 3875−3877.